Development 134, 2481-2489 (2007) doi:10.1242/dev.006346

Adenylyl cyclase-dependent axonal targeting in the olfactory system

Julien A. Dal Col[1,*], Tomohiko Matsuo[1,*], Daniel R. Storm[2] and Ivan Rodriguez[1,†]

The vertebrate olfactory bulb is a remarkably organized neuronal structure, in which hundreds of functionally different sensory inputs are organized into a highly stereotyped topographical map. How this wiring is achieved is not yet understood. Here, we show that the olfactory bulb topographical map is modified in adenylyl cyclase 3 (adenylate cyclase 3)-deficient mice. In these mutants, axonal projection targets corresponding to specific odorant receptors are disorganized, are no longer exclusively innervated by functionally identical axonal projections and shift dramatically along the anteroposterior axis of the olfactory bulb. Moreover, the cyclase depletion leads to the prevention of neuropilin 1 (Nrp1) expression in olfactory sensory neuron axonal projections. Taken together, our data point to a major role played by a crucial element of the odorant-induced transduction cascade, adenylyl cyclase 3, in the targeting of olfactory sensory neuron axons towards the brain. This mechanism probably involves the regulation of receptor genes known to be crucial in axonal guidance processes.

KEY WORDS: Olfaction, Axon guidance, Adenylyl cyclase 3, Mouse

INTRODUCTION

Daily tasks encountered by mammals, and crucial for their own survival or for that of their species (such as food localization or intergender interactions, for example), largely depend on a functional olfactory system. This latter is composed of two subsytems, with sensory parts, the vomeronasal and the main olfactory neuroepithelia, that are physically and at least partly functionally separated.

The first step in olfactory processing in the main olfactory system involves the recognition of chemical stimuli by odorant receptors. These are seven transmembrane proteins expressed on dendritic endings of olfactory sensory neurons (OSNs) (Buck and Axel, 1991). Each OSN expresses a single or a few odorant receptor genes among a repertoire of over a thousand in the mouse (Chess et al., 1994). Odorant receptor activation leads to a transduction cascade involving the G protein alpha subunit Gαolf, followed by the activation of adenylyl cyclase 3 (adenylate cyclase 3; Ac3) and the cAMP-dependent opening of an heteromeric cation permeable channel containing the Cnga2 subunit (Ronnett and Moon, 2002). Calcium entry into the OSN then activates a chloride current that helps to depolarize the neuron.

OSNs project their axons towards spherical neuropil-rich structures called glomeruli, located in the cortical layer of the olfactory bulb (Mombaerts et al., 1996; Vassar et al., 1994). To each functionally identical OSN population (i.e. expressing the same odorant receptor) correspond only two glomeruli per bulb. The topographical position of these two structures is conserved between the right and left bulbs, and between different individuals. Thus, the mouse olfactory bulb is composed of thousands of glomeruli, organized in a well-defined and relatively fixed topographical map.

[1]Department of Zoology and Animal Biology, and NCCR Frontiers in Genetics, University of Geneva, Geneva, Switzerland. [2]Department of Pharmacology, University of Washington, Seattle, WA 98195-7280, USA.

*These authors contributed equally to this work
†Author for correspondence (e-mail: Ivan.Rodriguez@zoo.unige.ch)

Accepted 13 April 2007

Unlike that observed for most mammalian neuronal structures, the wiring process leading to the establishment of this remarkable bulbar map is not limited to a narrow embryonic phase. Targeting of OSNs towards the bulb is indeed a lifelong continuous process, which compensates for the unusually (for neurons) short lifespan of OSNs.

How is this precise map elaborated and maintained? This process is not yet understood, but mounting evidence points to activity-dependent mechanisms (Yu et al., 2004; Zou et al., 2004). Odorant receptors (Mombaerts et al., 1996; Wang et al., 1998), G protein subunits (Imai et al., 2006) and Pka (Yoshida et al., 2002) have been reported to play a role in OSN targeting to the olfactory bulb. Two recent reports propose that odorant receptor-mediated signals direct axonal targeting of OSNs via the activation of its associated G protein and the production of cAMP (Chesler et al., 2007; Imai et al., 2006). However, analyses of mouse mutants lacking key elements of the odorant transduction cascade such as Gαolf or Cnga2 have failed to reveal major targeting defects of OSNs (Belluscio et al., 1998; Zhao and Reed, 2001; Zheng et al., 2000); except for Ac3, which has been linked to a disorganization of the glomerular layer in the bulb (Chesler et al., 2007; Trinh and Storm, 2003).

We report here that Ac3 is a likely key element in the odorant-receptor-mediated axonal guidance, as its lack drastically affects the reading of the olfactory bulb coordinates by OSN axonal projections, and prevents the expression of a major axon olfactory axon guidance molecule, neuropilin 1.

MATERIALS AND METHODS

Mice

Generation of *Ac3*$^{-/-}$, *P2* (*Olfr17*)*-lacZ*, *MOR23* (*Olfr16*)*-GFP*, *M72* (*Olfr160*)*-lacZ*, *Omp-lacZ*, *Omp-GFP* and *V1rb2-lacZ* mice has been previously described (Feinstein and Mombaerts, 2004; Mombaerts et al., 1996; Potter et al., 2001; Vassalli et al., 2002; Wong et al., 2000; Rodriguez et al., 1999). Mice were bred on a C57BL6 background and animals analyzed were issue from Ac3$^{+/-}$ crosses. Age- and sex-matched littermates were used when comparing mutant and wild-type phenotypes. Animals were housed and handled in accordance with the guidelines and regulations of the institution and of the state of Geneva.

In situ hybridizations

Tissues were embedded in OCT without fixation, and 14 μm cryostat slices were mounted on Superfrost+ slides (Menzel-Glaser), dried for 40 minutes, fixed for 20 minutes at 4°C with 4% paraformaldehyde and hybridized overnight at 65°C in the following buffer: 1× salt buffer (10 mM NaCl, 5 mM $NaH_2PO_4·H_2O$, 5 mM $Na_2HPO_4·2H_2O$, 5 mM EDTA, pH 7.5), 50% formamide, 10% dextran sulphate, 1 μg/μl tRNA, 1× Denhardt's, with 20 ng/μl cRNA probe(s). The Ac3 probe contained a 604 bp fragment starting 60 bp before the start codon. For *M72* (*Olfr160*; *M72-lacZ*) and *P2* (*Olfr17*; *P2-lacZ*), or *MOR23* (*Olfr16*; *MOR23-GFP*) and *Omp* (*Omp-GFP*) transcript identification, probes containing a 1.8 kb *Hin*dIII fragment of *lacZ* or the entire GFP ORF were used, respectively. Following hybridizations, slides were washed twice at 65°C and once at RT with 1× SSC, 50% formamide and 0.1% Tween 20. Slides were pre-incubated in 1× MABT, 2% blocking reagent (Roche) for 30 minutes followed by a 1 hour incubation with alkaline phosphatase-anti-digoxigenin antibody (1:1000, Roche) or/and peroxidase-anti-fluorescein antibody (1:200, Roche). Peroxidase activity was revealed by washing slides three times with TNT (150 mM Tris, 150 mM NaCl, 0.05% Tween 20, pH 7.5), incubation for 30 minutes with a biotinyl-tyramide solution (PerkinElmer, 1:50), three washes with TNT and incubation for 30 minutes with streptavidin-Alexa 488 (Invitrogen, 1:100). Alkaline phosphatase activity was detected by incubating slides with Fast Red substrate (DAKO) for 30 minutes. Sections were mounted in DABCO mounting medium (Sigma). Fluorescein and digoxigenin-labeled RNA probes were prepared using the DIG RNA Labeling Kit (Roche) following the manufacturer's instructions.

Microscopy

Images were taken on a Zeiss Axioplan2 wide field microscope or on a Leica SP2 confocal microscope. All sections were counterstained with DAPI (5 minutes, 1 μg/ml) and slides were mounted using DABCO anti-fade mounting medium.

Whole-mount analyses

Animals were dissected, the heads fixed by immersion in 4% paraformaldehyde at 4°C for 20 minutes and stained with X-Gal as previously described (Rodriguez et al., 1999). Whole-mount images were taken on a Leica MZFLIII or Zeiss SteREO Lumar.V12 fluorescence-equipped binoculars.

RT-PCRs

Tissues were harvested and immediately processed using the Qiagen RNeasy Mini Kit. The following primers were used to amplify Ac3 transcripts: 5′-ATCCCAAATTCCGGGTCATCAC-3′ and 5′-GGAA-GCCGTACTCTCGAAGGAT-3′. Amplifications were performed under the following conditions: 5 minutes at 95°C, followed by 34 cycles of 1 minute at 95°C, 1 minute at 60°C, and 2 minutes at 72°C, and a final extension of 10 minutes at 72°C.

Western blots

Tissues were homogenized in 10 mM Tris-HCl (pH 7.6), 1 mM EDTA, 100 mM NaCl, 100 μg/ml PMSF, 1 μg/ml aprotinin. Protein extracts (15 μg) were loaded on 10% Bis-Tris NuPAGE gels (Invitrogen), and transferred to PVDF membranes. Membranes were incubated for 16 hours with an anti-Ac3 antibody (1:500, sc-588 Santa Cruz Biotechnology), followed by incubation with an alkaline phosphatase-conjugated anti-rabbit antibody. The phosphatase was revealed with the CDP-Star chemiluminescent substrate (WesternBreeze, Invitrogen).

Immunohistochemistry

Tissues were fixed for 2 hours (Ac3) or overnight (neuropilin 1, NCAM) in 4% paraformaldehyde and embedded in OCT. Cryostat slices (10-14 μm) were mounted on Superfrost+ slides. Slides were pre-incubated in 0.5% Triton, 10% FCS (except for anti-Ac3: 0.1% FCS), 1× PBS for 30 minutes at room temperature. Goat anti-rodent-Omp (1:200-800, Wako Laboratory Chemicals), rabbit anti-mouse-Ac3 (1:400, sc-588 Santa Cruz Biotechnology), mouse anti-rat NCAM (1:500, Sigma) and goat anti-rat-Neuropilin (1:100, AF566, R&D Systems) antibodies were used. After overnight incubation at 4°C, slides were washed three times with 0.5% Triton, 1× PBS for 10 minutes and stained with DAPI for 5 minutes (1 μg/ml). Primary antibodies were revealed with Alexa 488-conjugated donkey anti-goat (1:200-800, Invitrogen), Cy3-conjugated donkey anti-rabbit (1:250, Jackson Laboratories), Alexa 555-conjugated donkey anti-mouse (1:500, Invitrogen) or Alexa 555-conjugated donkey anti-goat (1:800, Invitrogen) secondary antibodies. Slides were mounted with antifade reagent (DABCO). To evaluate the specificity of the anti-Ac3 antibody, the peptide used to raise the antibody (Santa Cruz) was pre-incubated for 2 hours at room temperature with the Ac3 antibody [10× excess (w/w)].

RESULTS

Expression of Ac3 in the olfactory system

Ac3 is expressed by OSNs and is a main player in the odorant-induced transduction cascade (Wei et al., 1998; Wong et al., 2000). We found it present from embryogenesis to adulthood in OSNs, both at the mRNA (Fig. 1A,C), and protein levels (Fig. 1B,E-H). As expected, the protein was highly enriched in OSN dendritic endings (Fig. 1H), but was barely detectable in OSN somata. Surprisingly, immunohistochemical analysis of axonal projections comprising the nerve layer and glomeruli indicated that Ac3 was present in these structures (Fig. 1H), although at a lower concentration than the one observed in dendritic endings. Transcription of Ac3 by OSNs was observed from the early stages of OSN axonal pathfinding (Fig. 1A). The corresponding protein was also identified early during development, at embryonic day 12.5 (E12.5) in OSN dendrites and at E16 in the nerve layer (Fig. 1E).

Western blot analysis of Ac3 OSN and olfactory bulb extracts showed the absence of the major olfactory glycosylated Ac3 form in the bulb (200-210 kD) and the presence of another Ac3 variant, of lower apparent molecular weight (155-170 kD) (Fig. 1B). A short, possibly similar, Ac3 variant has previously been reported in male germ and smooth muscle cells (Gautier-Courteille et al., 1998; Wong et al., 2001).

We then investigated the possible Ac3 expression in sensory neurons pertaining to the vomeronasal system, a system that theoretically does not transduce chemosensory signals via cAMP. We found a weak expression of the Ac3 transcript in the vomeronasal neuroepithelium (Fig. 1D).

Ac3-deficient OSNs target aberrantly to the olfactory bulb

As previously mentioned, mice bearing null alleles of genes coding for the major elements of the odorant signal transduction cascade (Gαolf) exhibit, if any, only weak alterations of the topographical map in the olfactory bulb (Belluscio et al., 1998; Zhao and Reed, 2001; Zheng et al., 2000). These observations, supporting the argument against a role played by part of the odorant-induced cascade in guidance, possibly reflect a partial knockout rescue by molecules still present in OSNs, such as the ubiquitously expressed Gαs. To test this caveat, we investigated the potential axon guidance alterations resulting from the lack of Ac3 in OSNs.

To identify a potential global effect of the cyclase on the whole olfactory sensory population, we first visualized the entire OSN population and its axonal projections, by crossing a line deficient in Ac3 (Wong et al., 2000) and a transgenic mouse line (*Omp-lacZ*) in which all mature OSNs express β-galactosidase (Mombaerts et al., 1996). Whole-mount analyses of $Ac3^{-/-}$ olfactory bulbs showed a strikingly altered organization of glomeruli in the bulbs. In control animals, glomeruli cover the entire olfactory bulb and are often overlapping, rendering their individual identification in whole mounts difficult (Fig. 2A,C,D). The dorsocaudal part of the olfactory bulbs from P15 $Ac3^{-/-}$ animals were almost devoid of Omp-positive glomeruli (Fig. 2B,E,F), revealing some rare caudally located

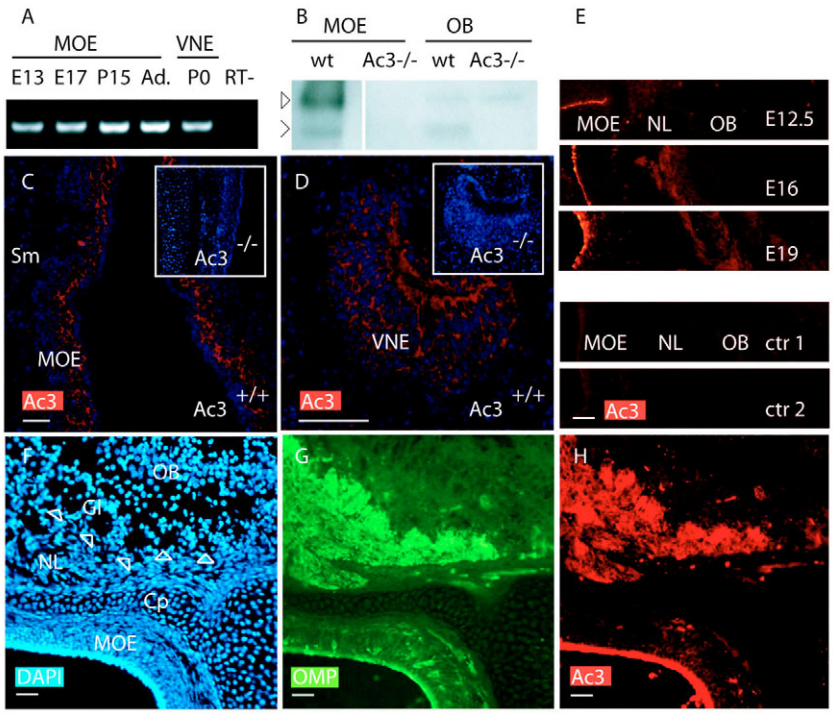

Fig. 1. Ac3 expression in the mouse olfactory system. (**A**) RT-PCR showing that Ac3 transcripts are present during development of the main olfactory and vomeronasal epithelia. (**B**) Western blot analysis of Ac3 expression in the main olfactory epithelium and olfactory bulb. The closed arrow indicates the position of the expected 200-210 kD Ac3 band. The open arrow indicates the Ac3 variant found in the olfactory bulb (155-170 kD). A weak non-specific band of 200 kD is present in wild-type and Ac3$^{-/-}$ olfactory bulb extracts. (**C**) In situ hybridization of the olfactory epithelium shows Ac3 mRNA expression in OSNs of a P15 mouse. A control hybridization on a similar section from an Ac3-null mouse is shown in the insert. (**D**) Expression of Ac3 in the vomeronasal organ of a P0 mouse (insert shows the corresponding in situ hybridization of an Ac3-null animal). The signal was weaker than the one observed in the main olfactory epithelium. (**E**) Expression of Ac3 in the olfactory system of E12.5, 16 and 19 embryos. The two lower images represent antibody controls: ctr1, Ac3$^{-/-}$ section; ctr2, pre-adsorbed antibody. (**F-H**) Immunohistochemistry (F, DAPI; G, OMP) on coronal sections shows that Ac3 (H) is highly enriched on OSN dendritic endings, but is also expressed on OSN axonal bundles and in glomeruli. Arrowheads in F show individual glomeruli. Scale bars: 60 μm. Cp, cribriform plate; Gl, glomerular layer; MOE, main olfactory epithelium; NL, nerve layer; OB, olfactory bulb; Sm, septum; VNE, vomeronasal epithelium.

glomeruli apparently unaffected and easily identifiable because of the absence of surrounding Omp-expressing glomeruli. Specific glomeruli, known as the necklace and Grueneberg glomeruli, which are located at the very caudal part of the olfactory bulb, appeared loosely organized in the mutants (Fig. 2E,F). Sagittal sections through olfactory bulbs confirmed that not only the global glomerular map was affected in Ac3 mutants, but also, at the glomerular level, the individual structure of glomeruli, which appeared disorganized (Fig. 2G,H).

OSNs located in different zones of the main olfactory neuroepithelium are known to project to different areas in the olfactory bulb (Mori et al., 2000). Did the glomerular map alteration observed in Ac3$^{-/-}$ animals reflect the absence of the OSN population projecting to the caudal part of the bulb? We analyzed by whole mounts the olfactory sensory area in *Omp-lacZ Ac3*$^{-/-}$ mice to identify potential zones devoid of Omp-expressing neurons, but did not identify any specific epithelium area lacking mature OSNs (Fig. 2A,B).

The weak Ac3 expression in the vomeronasal organ then led us to investigate a potential role, possibly similar to the one we observed in the main olfactory system, also played by this protein in the wiring of vomeronasal sensory neurons. We analyzed whole mounts of *Ac3*$^{-/-}$ *Omp-lacZ* accessory olfactory bulbs (10 bulbs from P10-P25 animals), but did not observe any major targeting alteration (Fig. 2C-F). Following this initial and relatively rough analysis of vomeronasal projections, we investigated potential finer topographical alterations of the axonal projection map in this system. Apically located vomeronasal sensory neurons are known to innervate 15 to 30 glomeruli (with a global position that is relatively fixed) in each accessory olfactory bulb (Belluscio et al., 1999; Rodriguez et al., 1999). To evaluate putative mis-wiring defects in this system, we made use of a reporter line we previously generated that allows the identification of axonal projections of sensory neurons expressing the pheromone receptor gene *V1rb2* (Rodriguez et al., 1999). No major targeting alteration of *V1rb2*-expressing neuron axonal projections was observed in Ac3-null animals (Fig. 3J,K).

Anteroposterior glomerular shift in Ac3-deficient OSNs

To explain the lack of glomeruli on the caudal part of the main olfactory bulb, we hypothesized a potential mistargeting of OSNs to inadequate areas, or alternatively, and more simply, the non-innervation of the bulb by OSNs expressing specific receptors.

We tested these two possibilities by using three gene-targeted mouse lines, each allowing the identification of different and defined odorant-expressing OSNs, and most importantly, of their axonal projections up to their glomerular targets. We selected the *P2-lacZ* (Mombaerts et al., 1996), *MOR23-GFP* (Vassalli et al., 2002) and *M72-lacZ* (Feinstein and Mombaerts, 2004) knock-in lines,

corresponding to OSNs located in different neuroepithelial zones in the nasal cavity, and projecting to very different areas of the main olfactory bulb.

Wild-type P2-expressing OSNs form two glomeruli per bulb, rostroventrally (Mombaerts et al., 1996). The glomerular positions are, as is the rule for mammalian glomeruli, relatively fixed between animals. In the *P2-lacZ* reporter line, the medial glomerulus is readily visualizable on whole-mount views of the medial side of the bulb (Fig. 3A). No glomeruli innervated by P2-expressing OSNs were found in Ac3 mutant animals (nine P15 bulbs analyzed), despite the presence of P2-expressing OSNs sending axons towards the bulbs (Fig. 3B). In older animals (after P19), a small and weakly labeled medial glomerulus was rarely observed (data not shown). The global intensity of the β-galactosidase staining being weaker in the mutant animals (Fig. 3A,B), and the staining intensity being relatively comparable at the single cell level, we compared the number of P2-expressing OSNs in wild-type and Ac3$^{-/-}$ turbinates. We counted, using whole mounts, all P2-positive OSNs present on a well-circumscribed zone: the largest turbinate. As no particular clustering of P2-expressing OSNs was observed (within their expression zone), we considered these counts representative of the total number of P2-expressing OSNs. We found 486±46 and 118±16 OSNs in wild-type and mutant animals respectively, indicating a drastic reduction of P2-expressing OSNs in Ac3$^{-/-}$ animals.

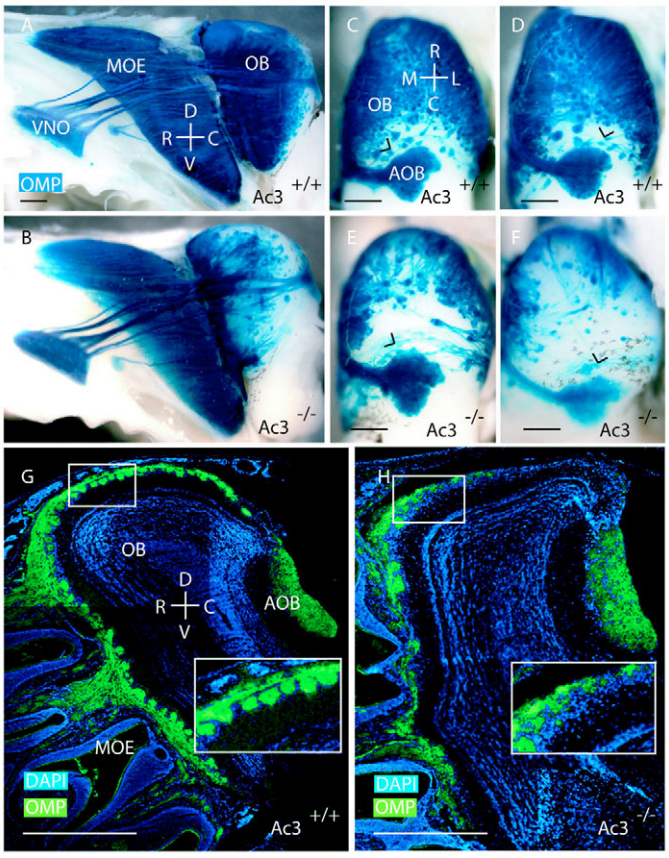

Fig. 2. Aberrant OSN projections in Ac3-null mice. (**A-F**) Whole-mount analysis of P15 *Omp-lacZ* bulbs in which all mature OSNs are stained blue. (A,B) Control and Ac3$^{-/-}$ mice, respectively. A clear reduction in the number of caudal glomeruli is observable in the mutant when compared with the control. (C,D) Dorsal view of the olfactory bulb of two animals. (E,F) Corresponding dorsal view of Ac3$^{-/-}$ animals, revealing a drastic reduction of dorsocaudally located glomeruli. Arrows indicate the position of necklace/Grueneberg glomeruli, the organization of which appears affected in the mutants. (**G**,**H**) Sagittal sections of control (G) and Ac3-null (H) P15 mice. Omp is stained in green. The complete lack of caudal Omp-positive glomeruli on the dorsal part of the bulb is clearly visible. Inserts correspond to high magnifications of wild-type and Ac3$^{-/-}$ dorsorostral glomerular layers, and show a glomerular disorganization in Ac3$^{-/-}$ animals. Scale bars: 0.5 mm. AOB, accessory olfactory bulb; C, caudal; D, dorsal; L, lateral; M, medial; MOE, main olfactory epithelium; OB, olfactory bulb; R, rostral; V, ventral; VNO, vomeronasal organ.

Wild-type M72 axonal fibers form two glomeruli per bulb, dorsocaudally (Fig. 3C,F) (Potter et al., 2001). Ac3 mutant animals exhibited a very low number of axonal projections at the topographical coordinates usually chosen by wild-type fibers to generate a large glomerulus. These projections formed, if any, one to four small glomerular-like structures (Fig. 3D). This phenotype was observed on both medial and lateral sides of the bulbs (Fig. 3G). Strikingly, two large and novel bilaterally symmetrical glomeruli innervated by M72-expressing axons were observed on the very rostral part of the bulb (21 wild-type and 29 Ac3$^{-/-}$ P15 bulbs analyzed) (Fig. 3D,E,G; Fig. 4A,B). The majority of M72-expressing OSN projections did therefore form two completely novel glomeruli. Histological analysis of bulbs showed that these M72 glomeruli were structurally altered and not exclusively innervated by fibers expressing the M72 receptor (Fig. 5B), confirming and expanding the results obtained with the rough analysis of *Omp-lacZ Ac3*$^{-/-}$ animals. We then counted the number of M72-expressing OSNs in Ac3$^{-/-}$ and wild-type mice, using again the largest turbinate as an easily identifiable window. We found 213±51 and 197±40 M72-expressing OSNs in mutant and wild-type animals, respectively, indicating, in contrast to that observed for the P2 receptor, an unaltered M72-expressing population size.

Axonal projections of wild-type MOR23-expressing OSNs end up on the medial side of the olfactory bulb, in a centrally located medial glomerulus (Fig. 3H) (Vassalli et al., 2002). Ac3 mutant animals exhibited, similarly to the situation observed for M72 axonal fibers, rare axons reaching the location in the bulb innervated by MOR23-expressing OSNs in wild-type animals (three P15 bulbs analyzed) (Fig. 3I). Again, as observed for M72-expressing OSNs, completely novel glomeruli were formed on the rostral part of the bulb (Fig. 3I), receiving input from most of the MOR23-expressing OSN population. These new glomeruli were not always well defined (Fig. 3I; Fig. 5A), and their boundaries were difficult to identify even histologically due to a loose ensheathing by periglomerular cells (Fig. 5A).

We plotted the precise position of 121 and 34 glomeruli corresponding to M72- and MOR23-expressing fibers, respectively (Fig. 4A-C). A clear anteroposterior shift was observed for glomeruli innervated by MOR23 and by M72 OSN projections. The positions of the novel glomeruli were conserved between bulbs and between animals, except for dorsomedial M72 glomeruli, which were relatively variable in position (Fig. 4B).

Choice of a glomerulus

Schematically, in wild-type animals, OSNs located in the neuroepithelium of the nasal septum target to glomeruli located on the medial part of the olfactory bulb, while those located on turbinates target to the lateral side of the bulb. We report here that some OSNs lacking Ac3 expression, despite the innervation of a novel glomerulus by the majority of their apparently functionally identical neighbors, still project to a location corresponding to the area innervated by wild-type OSNs. Are there differences between M72-expressing OSNs targeting to one or other of the glomeruli?

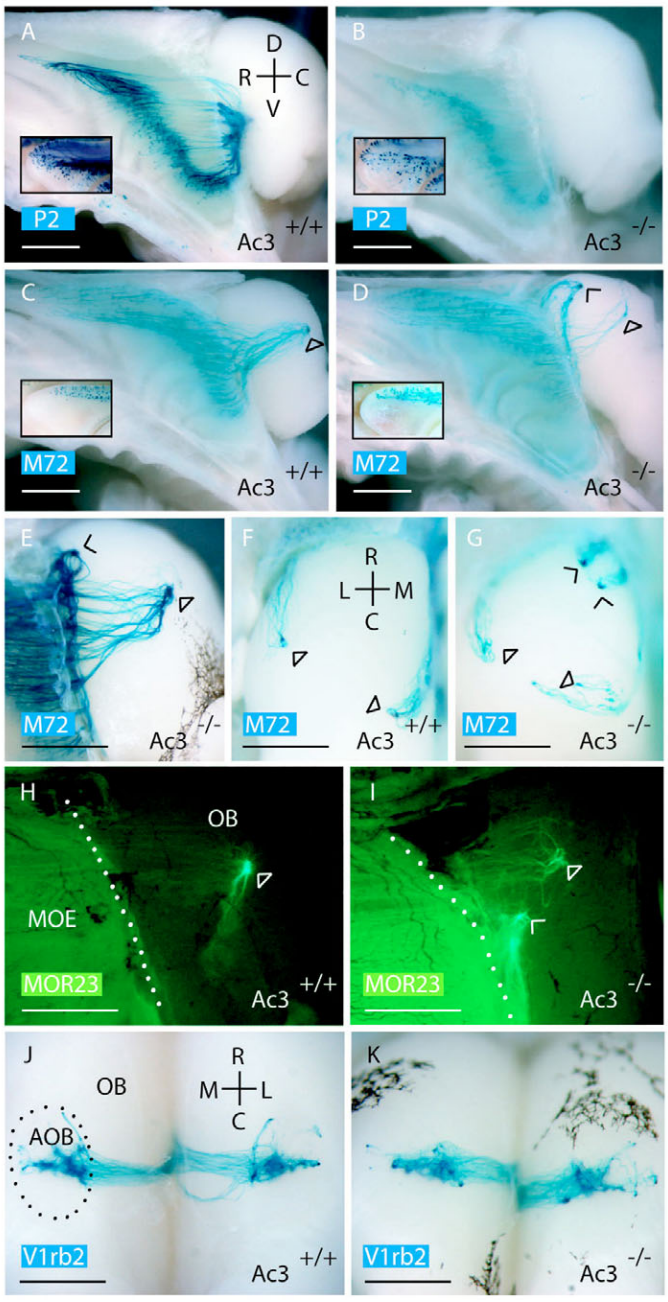

Fig. 3. Axonal projections of P2-, M72-, MOR23- and V1rb2-expressing Ac3$^{-/-}$ sensory neurons. (**A-K**) Whole-mount views of X-Gal-stained (blue) OSNs (except for H and I, in which the green color reflects the expression of GFP). (A,B) No glomerulus is observed in B. Inserts show the tip of the largest right turbinates of wild-type and Ac3$^{-/-}$ mice. The number of P2-expressing OSNs is reduced in mutant animals. (C,D) Lateral view of P15 *M72-lacZ* control and Ac3$^{-/-}$ animals. Closed arrows indicate the position of the wild-type medial glomeruli. The open arrow indicates the position of the novel, rostromedial glomerulus. Analysis of turbinates (inserts) shows no differences in the number of M72-expressing neurons. (E) The two medial glomeruli persist in Ac3$^{-/-}$ *M72-lacZ* P50 mice. (F,G) Dorsal views of P15 *M72-lacZ* (F) control, and (G) Ac3$^{-/-}$ left bulbs. Open and closed arrows indicate the topographical position of mutant and wild-type M72 glomeruli, respectively. (H,I) Medial views of right bulbs of P15 animals, in which all axonal projections corresponding to MOR23-expressing OSNs are GFP fluorescent. A novel glomerulus is formed on the rostroventral side of the bulb in Ac3 mutant animals (open arrow). (J,K) Dorsal views of the accessory olfactory bulb of *V1rb2-lacZ* control (J) and Ac3-null (K) 3-week-old animals. External boundaries of the left accessory olfactory bulb are shown as a dotted line in J. No obvious alteration of the typical V1rb2 map was observed. Scale bar: 1 mm. C, caudal; D, dorsal; L, lateral; M, medial; R, rostral; V, ventral.

These differences could reside in a variable dependence on Ac3 between OSNs expressing the same odorant receptor gene. Depending on the time (during embryogenesis or later after birth) at which an OSN was born, its Ac3 dependence could be unequal. We did observe the formation of ectopic MOR23 and M72 glomeruli in newborn and adult animals of various ages (Fig. 3D,E), supporting the argument against this hypothesis.

Alternatively, formation of novel glomeruli could be the result of a positional alteration occurring upstream of the bulbar phenotype. It is known that neuroepithelium zones in which OSN cell bodies are located affect the position of their corresponding glomeruli in the olfactory bulb. To test this possibility, and taking advantage of the fine genetic tools represented by the knock-in lines, we analyzed, similarly to what we previously described for *Omp-lacZ* mice, the zonal distribution in the olfactory epithelium of M72-expressing OSNs, and their corresponding zonal distribution in Ac3-null animals. We did not find any positional shift of OSN cell bodies in the neuroepithelium between wild-type and mutant animals (Fig. 4D).

We then investigated the possibility that some OSNs could be dependent, or independent, on Ac3 expression, a situation that could be reflected by their expression, or non-expression, of Ac3. A clear gradient of Ac3 transcripts was observed by in situ hybridization in the main olfactory neuroepithelium, with apical OSNs more reactive than basal ones (Fig. 1C; Fig. 6A,C). We evaluated Ac3 transcription in OSNs expressing M72 (Fig. 6A-C), MOR23 or P2 in P4-P5 animals. Surprisingly, we found 60 (M72), 71 (MOR23) and 68% (P2) of OSNs in which we were unable to detect Ac3 transcripts (393 MOR23, M72 or P2 OSNs analyzed; Fig. 6D). It should be noted that a lack of signal by in situ hybridization does not necessarily indicate a complete lack of transcription. These Ac3-negative OSNs were mostly located in the most basal part of the neuroepithelium. To investigate the degree of differentiation of these two Ac3 high and low expressors, we performed double in situ hybridizations with an Ac3 probe and a probe recognizing Omp transcripts (which are specifically expressed in mature OSNs) (Fig. 6E,F). We found that over 90% of the Ac3 strongly positive OSNs were also positive for Omp, indicating a relatively advanced degree of differentiation, and suggesting that our identification of two Ac3-expressing populations reflects the maturation stage of OSNs. In conclusion, OSNs expressing an identical receptor represent a non-homogenous population, and can express different levels, or different variants of Ac3 transcripts; but the link, if any, between these two populations and the two targeting options is still lacking.

Lack of neuropilin 1 expression in Ac3$^{-/-}$ OSN projections

Neuropilin 1 is a semaphorin class 3 receptor. A relatively large population of OSNs projecting to the medial and lateral parts of the olfactory bulb expresses neuropilin 1 (Schwarting et al., 2000). Both neuropilin 1 and its ligand Sema-3A have been reported to

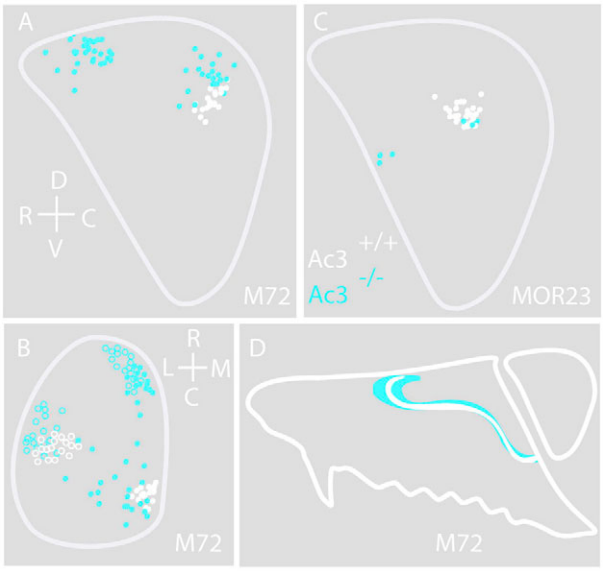

Fig. 4. Anteroposterior targeting shift in P15 Ac3-null mice. (**A**) Schematic diagram showing the medial portion of the right bulb. White dots correspond to the topographical glomerular coordinates innervated by M72-expressing OSNs. Blue dots indicate the innervation of M72-expressing OSNs in an Ac3$^{-/-}$ background. (**B**) Schematic showing a dorsal view of a left olfactory bulb. The color code is similar to that in A, and circles indicate lateral glomeruli. (**C**) Similar lateral view to that in A, but with coordinates corresponding to glomeruli innervated by MOR23-expressing OSNs. (**D**) Lateral schematic view of the olfactory system, in which is indicated the zonal limit reached on the septum by M72-expressing OSNs in Ac3$^{+/+}$ mice; in blue is the corresponding limit reached in Ac3$^{-/-}$ animals. C, caudal; D, dorsal; L, lateral; M, medial; R, rostral; V, ventral.

play a role in axon guidance processes in the olfactory bulb (Pasterkamp et al., 1998). Moreover, a single cell cDNA library from an OSN expressing an olfactory receptor unable to couple to G proteins was reported to lack neuropilin 1 transcripts (Imai et al., 2006). We therefore investigated if a potential alteration of neuropilin 1 expression was associated with the lack of Ac3 expression.

Neuropilin 1 expression in the olfactory bulb starts on the rostrolateral side of the bulb, and progresses towards the medial side on more caudal parts (Schwarting et al., 2000). Parasagittal sections of olfactory bulbs indicated that neuropilin 1 expression was completely absent in axonal bundles and nerve layer in Ac3$^{-/-}$ mice (Fig. 7A,B). Coronal sections through the olfactory bulbs showed a lack of neuropilin 1 in glomeruli from mutant mice, despite the presence of sensory neuron projections (Fig. 7D).

We then determined, in wild-type animals, the potential expression of neuropilin 1 in glomeruli innervated by MOR23-expressing OSNs. A strong expression was observed in MOR23 axonal fibers forming both lateral (Fig. 7E-G) and medial (Fig. 7H-J) glomeruli. The same analysis was performed with medial and lateral M72 and P2 glomeruli. Expression of neuropilin 1 was observed in M72 glomeruli (Fig. 7M,N), whereas none was found in P2 glomeruli (Fig. 7K,L) (Schwarting et al., 2004).

DISCUSSION

cAMP as a major player in OSN axonal guidance

Our report points to a major role played by Ac3, a crucial element of the odorant transduction cascade, in the wiring of the rodent olfactory bulb.

Apparently, most members of the olfactory transduction cascade (including the odorant receptor, the G protein and Ac3) are not only present at the OSN dendritic endings, which are in contact with the outside world, but are also observed on the OSN axonal projections, which leave the nasal cavity and enter the olfactory bulb. In light of this observation, it is naturally tempting to consider this cascade at the core of the readout mechanism allowing a growth cone to find an adequate target. The topographical position of a given glomerulus would thus primarily depend on the odorant receptor it expresses, as it is possibly the only molecule by which a neuronal population innervating a given glomerulus differs from the one innervating the neighboring one. This is to be paralleled with the conclusions of two very recent reports indicating that expression of a constitutively active Gαs subunit or overexpression of a dominant-negative Pka in OSNs, leads to a shift of glomeruli innervated by I7-expressing fibers along the anteroposterior axis of the olfactory bulb (Chesler et al., 2007; Imai et al., 2006).

If the odorant-induced cascade is involved in axonal guidance mechanisms, why is Ac3 the only member of the olfactory transduction cascade for which deletion leads to a drastic modification of the wiring diagram in the olfactory bulb? First, it is likely that only the first steps of the odorant-induced transduction cascade (i.e. up to the production of cAMP) are involved in guidance mechanisms. Second, redundancy in the system could allow, for example, to compensate for the lack of Gαolf by the expression of

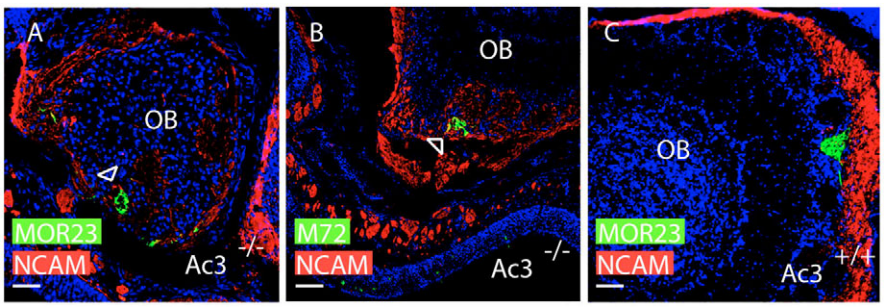

Fig. 5. Altered structure and non-exclusive innervation of glomeruli in Ac3$^{-/-}$ glomeruli. (**A**,**B**) Sagittal sections through olfactory bulbs of P17 Ac3$^{-/-}$ MOR23 and M72 homozygous mice. Arrows indicate the presumed external glomerular limits, which are difficult to identify due to the loose ensheathing of the glomeruli by periglomerular cells. The glomerular structures are irregular, and the glomeruli corresponding to M72 and MOR23 are innervated by fibers stained with NCAM (in red) that do not express M72 or MOR23. Control sections of wild-type glomeruli innervated by MOR23 (**C**) or M72 fibers show exclusive innervation and regular structure of the glomeruli (data not shown) (Feinstein and Mombaerts, 2004; Vassalli et al., 2002). Scale bars: 100 μm. OB, olfactory bulb.

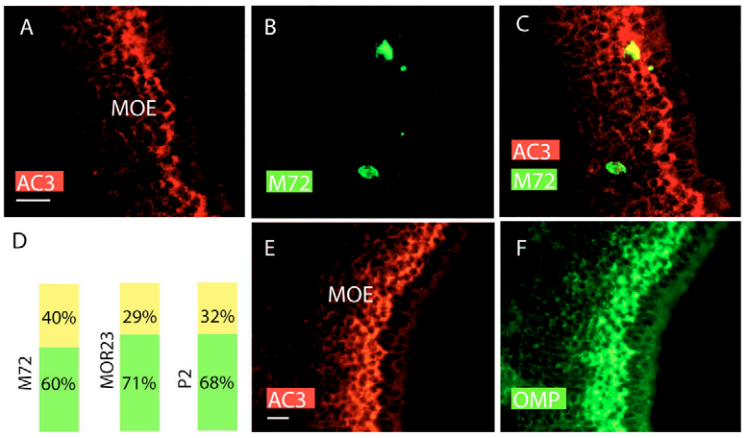

Fig. 6. Ac3/OR co-expression in the olfactory neuroepithelium. (**A-C**) In situ hybridizations of main olfactory epithelium sections (*M72-lacZ* P5 mouse), with an Ac3 probe (red) and a probe recognizing M72-expressing OSNs (β-gal, green). Two M72-expressing OSNs are shown in C, one positive and the other negative for Ac3 expression. (**D**) Graph indicating the percentage of MOR23-, M72- and P2-expressing OSNs reactive (yellow) or not (green) with the Ac3 probe. (**E**,**F**) In situ hybridizations corresponding to Ac3 (red) and Omp (green) expression. A clear correlation of expression can be observed. Scale bars: 30 μm. MOE, main olfactory epithelium.

Gαs, a subunit also present in OSNs that is phylogenetically and functionally (i.e. activating adenylyl cyclases) highly related to Gαolf. Such compensatory mechanisms have previously been observed between Gα subunits (Offermanns and Simon, 1998).

The same logic of redundancy can be applied to our inability to find wiring defects in vomeronasal sensory neuron projections. Indeed, in this last tissue, adenylyl cyclase 2 is highly expressed.

A cautionary note should be added here. If cAMP signals direct all axonal targeting of OSNs, why do we still observe, at least in some parts of the olfactory bulb, apparently relatively unaffected glomeruli? Redundant adenylyl cyclases could again come to the rescue, but it is as likely that other mechanisms independent of cAMP levels are at work.

Ac3-dependent and -independent OSN targeting

Our data show that OSNs expressing an identical odorant receptor (M72 or MOR23) and lacking Ac3, target to novel, rostrally located glomeruli. However, a non-negligible and consistent proportion of the OSN population still targets to topographical positions similar to those observed in wild-type animals (this does not necessarily mean that these fibers reached this position by reading the same axon guidance cues that wild-type fibers usually do). How can we explain this surprising situation?

First, the modification of the bulbar topographical map could reflect the alteration of the upstream map, i.e. the zonal restriction of OSNs in the olfactory epithelium. Our data do not support this hypothesis.

Second, one could imagine that, depending on the position of a given OSN (on the rostroapical part of turbinate 2 versus on the caudoventral portion of another turbinate, for example), the path and the signaling cues that will lead their projections to the bulb are different. Thus, it is possible that for a given OSN, depending on its position, the signal encountered during the wiring process requires or does not require Ac3 function.

Alternatively, one could propose that OSN targeting to the bulb during early development or later is unequally dependent on Ac3, despite the fact that comparison of adult and newborn topographical maps does not show a consistent difference between axonal projection patterns.

Finally, two OSN populations, dependent or not on Ac3 expression, could be constitutively present in the nasal cavity. We found a large proportion of Omp-negative OSNs expressing the odorant receptors M72, P2 or MOR23 containing, if any, very low levels of Ac3 transcripts. As odorant receptor transcription is a sign of OSN relative maturity, one would expect that the expression of molecules involved in guidance mechanisms should precede or be concomitant with odorant receptor expression. Our observations do therefore not rule out the existence of Ac3-dependent and independent wiring requirements for OSNs expressing the same odorant receptor.

Ac3 and glomerular formation

In addition to the glomerular map alterations resulting from the lack of Ac3, we also report important perturbations in the formation of glomeruli. We indeed observed glomeruli corresponding to M72 co-innervated by OSNs not expressing M72, and therefore probably expressing other receptors. This situation is very different from the one encountered in wild-type animals, in which glomeruli, even if receiving inputs from OSNs expressing barely different odorant receptors, do not commingle (Feinstein and Mombaerts, 2004). The alteration of glomerular formation in Ac3 mutants is even more pronounced for OSNs expressing the P2 receptor, as they are often unable to form glomeruli. This could, however, result from a known phenomenon, termed interdependence: a positive correlation exists between the number of OSNs expressing a given odorant and the probability of maintaining glomerular convergence (Ebrahimi and Chess, 2000). As we observed a drastic decrease in the number of P2-expressing OSNs in Ac3 mutant animals, the inability to form P2 glomeruli could simply result from a side effect affecting cell numbers.

In conclusion, Ac3 apparently plays a dual role, both in the formation of a functionally homogenous glomerulus, and in its global positioning.

A link between Ac3 and neuropilin 1

We report here a drastic modulation of neuropilin 1 expression in Ac3-deficient OSN projections. We do not know whether the phenotype we observe is a direct result of the lack of neuropilin 1. But neuropilin 1 expression pattern in wild-type animals and experimental evidence indicating its involvement in OSN guidance mechanisms suggest a functional link between Ac3, neuropilin 1 and rostrocaudal coordinates in the olfactory bulb. Moreover, Semaphorin-3A, a chemorepellent protein secreted by ensheathing glial cells in the nerve layer of the olfactory bulb, is an agonist of neuropilin 1 and is known to be involved in the targeting of OSNs to the olfactory bulb (Pasterkamp et al., 1998; Schwarting et al., 2000; Taniguchi et al., 2003). A definitive answer to this question will require a conditional neuropilin 1-null allele, because neuropilin 1 knockout mice die early during embryogenesis (Takashima et al., 2002).

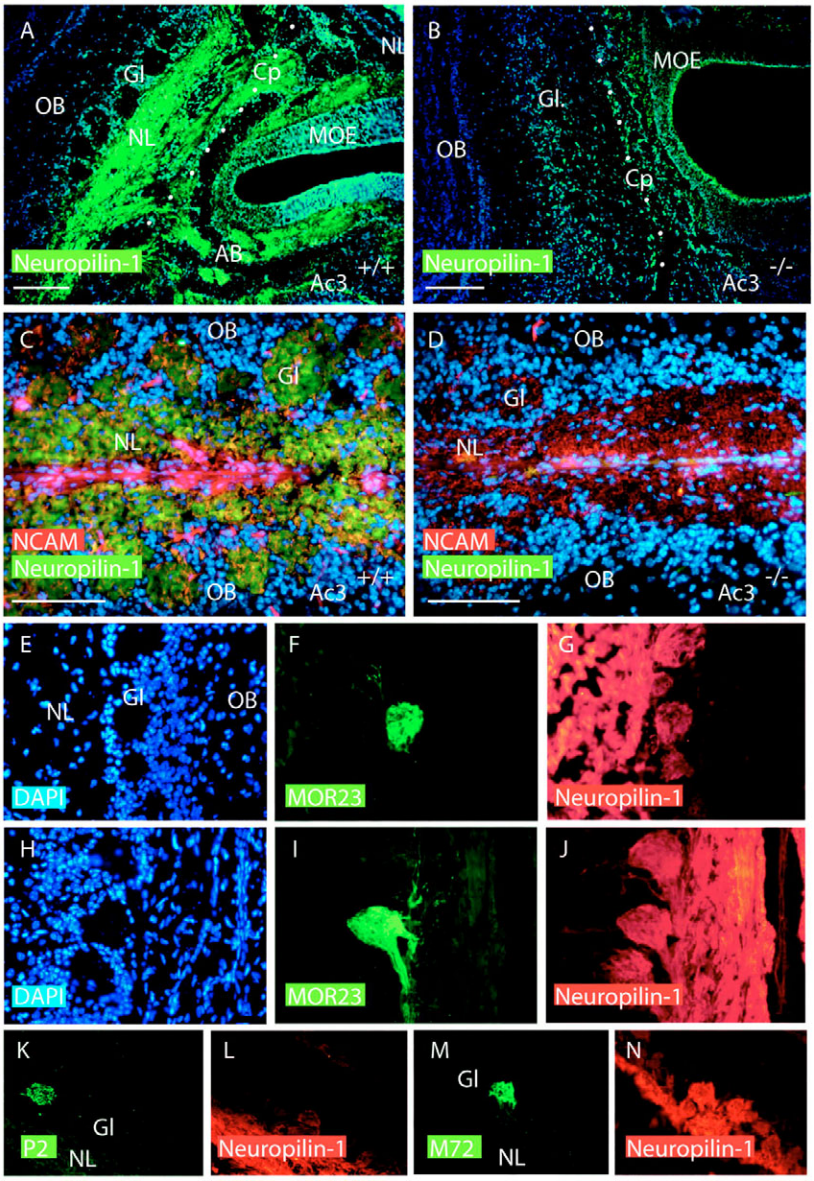

Fig. 7. Neuropilin expression in Ac3$^{-/-}$ and Ac$^{+/+}$ OSN axonal projections. (**A**) Sagittal section through the olfactory system of a P20 control mouse shows a strong neuropilin 1 expression in OSN axonal bundles (AB) and in the nerve layer (NL) of the olfactory bulb. The cribriform plate is shown with white dots. (**B**) Similar staining as in A, on an Ac3$^{-/-}$ P20 mouse. No neuropilin 1 was detected in OSN axonal bundles and projections to the bulb. (**C**,**D**) Anti-neuropilin 1 staining (green) of Ac3$^{+/+}$ (C) and Ac3$^{-/-}$ (D) olfactory bulb coronal sections. No neuropilin 1 staining is observed in Ac3$^{-/-}$ nerve layer or glomeruli. NCAM-expressing OSN projections are in red. (**E-J**) Coronal sections of wild-type bulbs (P11) showing neuropilin 1 expression (red) in axonal projections corresponding to OSNs expressing the MOR23 odorant receptor (green). (E,H) DAPI staining. Both lateral (E-G) and medial (H-J) glomeruli are immunoreactive. (**K-N**) M72 (M) and P2 (K) glomeruli are respectively positive and negative for neuropilin 1 expression shown in N and L, respectively. Scale bars: 120 μm. Cp, cribriform plate; D, dorsal; Gl, glomerular layer; L, lateral; M, medial; NL, nerve layer; OB, olfactory bulb; V, ventral.

As MOR23- and M72-expressing OSNs are neuropilin 1-positive, one may easily suggest a linear link between the misexpression of Neuropilin1 in Ac3 mutants and the MOR23 and M72 mis-wiring defects. But then why are neuropilin 1-negative glomeruli, such as P2, also strongly affected by the lack of Ac3? First, Ac3 function may not only interfere with the expression of neuropilin 1, but also with other guidance cues, still to be identified and potentially involved in the wiring of P2-expressing fibers. Supporting this explanation, projections of P2-expressing OSN fibers have been found to be in a Sema-3A$^{-/-}$ background abnormally distributed in the bulb and converging to atypical places (Schwarting et al., 2004; Taniguchi et al., 2003). This phenotype, different from the one we report here in Ac3-null mice, supports the idea that our observations do not result exclusively from neuropilin 1 inhibition. Second, considering the dramatic shift of a large number of glomeruli towards the rostral parts of the bulb, the position and possibly the establishment of glomeruli that would normally be located at this position will probably be affected. Thus, a possible competition for permissive target areas may take place in the rostral parts of the bulb, and explain the indirect mistargeting of OSN fibers pertaining to OSNs not expressing neuropilin 1. Third, as discussed previously, the lack of glomerular formation by Ac3$^{-/-}$ P2 fibers may simply reflect a too low number of P2-expressing neurons, and therefore not represent, unlike MOR23 and M72 projections, an adequate tool to study the role of Ac3 in guidance mechanisms.

Our understanding of neuronal navigation is progressing rapidly (Song and Poo, 2001), but large gaps are still remaining. Parallels between signaling pathways that allow growth cones to adequately react to their surroundings, and those involved in guidance of non-neuronal structures such as vascular networks, for example (Carmeliet and Tessier-Lavigne, 2005), have already emerged. These, including the recognition of cyclic nucleotides as key elements in transduction cascades, will surely soon be expanded, and provide a integrative understanding of neuronal guidance mechanisms.

We thank Martina Scotti for technical help, Peter Mombaerts, Anne Vassalli and Paul Feinstein for *Omp-lacZ*, *M72-lacZ*, *P2-lacZ* and *MOR23-GFP* mice, and Pierre Vassalli for comments on the manuscript. T.M. was supported by a Toyobo Foundation postdoctoral fellowship. This work was supported by grants from the Swiss National Science Foundation and the EMBO YIP.

References

Belluscio, L., Gold, G. H., Nemes, A. and Axel, R. (1998). Mice deficient in G(olf) are anosmic. *Neuron* **20**, 69-81.

Belluscio, L., Koentges, G., Axel, R. and Dulac, C. (1999). A map of pheromone receptor activation in the mammalian brain. *Cell* **97**, 209-220.

Buck, L. and Axel, R. (1991). A novel multigene family may encode odorant receptors: a molecular basis for odor recognition. *Cell* **65**, 175-187.

Carmeliet, P. and Tessier-Lavigne, M. (2005). Common mechanisms of nerve and blood vessel wiring. *Nature* **436**, 193-200.

Chesler, A. T., Zou, D. J., Le Pichon, C. E., Peterlin, Z. A., Matthews, G. A., Pei, X., Miller, M. C. and Firestein, S. (2007). A G protein/cAMP signal cascade is required for axonal convergence into olfactory glomeruli. *Proc. Natl. Acad. Sci. USA* **104**, 1039-1044.

Chess, A., Simon, I., Cedar, H. and Axel, R. (1994). Allelic inactivation regulates olfactory receptor gene expression. *Cell* **78**, 823-834.

Ebrahimi, F. A. and Chess, A. (2000). Olfactory neurons are interdependent in maintaining axonal projections. *Curr. Biol.* **10**, 219-222.

Feinstein, P. and Mombaerts, P. (2004). A contextual model for axonal sorting into glomeruli in the mouse olfactory system. *Cell* **117**, 817-831.

Gautier-Courteille, C., Salanova, M. and Conti, M. (1998). The olfactory adenylyl cyclase III is expressed in rat germ cells during spermiogenesis. *Endocrinology* **139**, 2588-2599.

Imai, T., Suzuki, M. and Sakano, H. (2006). Odorant receptor-derived cAMP signals direct axonal targeting. *Science* **314**, 657-661.

Mombaerts, P., Wang, F., Dulac, C., Chao, S. K., Nemes, A., Mendelsohn, M., Edmondson, J. and Axel, R. (1996). Visualizing an olfactory sensory map. *Cell* **87**, 675-686.

Mori, K., von Campenhause, H. and Yoshihara, Y. (2000). Zonal organization of the mammalian main and accessory olfactory systems. *Philos. Trans. R. Soc. Lond. B Biol. Sci.* **355**, 1801-1812.

Offermanns, S. and Simon, M. I. (1998). Genetic analysis of mammalian G-protein signalling. *Oncogene* **17**, 1375-1381.

Pasterkamp, R. J., De Winter, F., Holtmaat, A. J. and Verhaagen, J. (1998). Evidence for a role of the chemorepellent semaphorin III and its receptor neuropilin-1 in the regeneration of primary olfactory axons. *J. Neurosci.* **18**, 9962-9976.

Potter, S. M., Zheng, C., Koos, D. S., Feinstein, P., Fraser, S. E. and Mombaerts, P. (2001). Structure and emergence of specific olfactory glomeruli in the mouse. *J. Neurosci.* **21**, 9713-9723.

Rodriguez, I., Feinstein, P. and Mombaerts, P. (1999). Variable patterns of axonal projections of sensory neurons in the mouse vomeronasal system. *Cell* **97**, 199-208.

Ronnett, G. V. and Moon, C. (2002). G proteins and olfactory signal transduction. *Annu. Rev. Physiol.* **64**, 189-222.

Schwarting, G. A., Kostek, C., Ahmad, N., Dibble, C., Pays, L. and Puschel, A. W. (2000). Semaphorin 3A is required for guidance of olfactory axons in mice. *J. Neurosci.* **20**, 7691-7697.

Schwarting, G. A., Raitcheva, D., Crandall, J. E., Burkhardt, C. and Puschel, A. W. (2004). Semaphorin 3A-mediated axon guidance regulates convergence and targeting of P2 odorant receptor axons. *Eur. J. Neurosci.* **19**, 1800-1810.

Song, H. and Poo, M. (2001). The cell biology of neuronal navigation. *Nat. Cell Biol.* **3**, E81-E88.

Takashima, S., Kitakaze, M., Asakura, M., Asanuma, H., Sanada, S., Tashiro, F., Niwa, H., Miyazaki, J.-i., Hirota, S., Kitamura, Y. et al. (2002). Targeting of both mouse neuropilin-1 and neuropilin-2 genes severely impairs developmental yolk sac and embryonic angiogenesis. *Proc. Natl. Acad. Sci. USA* **99**, 3657-3662.

Taniguchi, M., Nagao, H., Takahashi, Y. K., Yamaguchi, M., Mitsui, S., Yagi, T., Mori, K. and Shimizu, T. (2003). Distorted odor maps in the olfactory bulb of semaphorin 3A-deficient mice. *J. Neurosci.* **23**, 1390-1397.

Trinh, K. and Storm, D. R. (2003). Vomeronasal organ detects odorants in absence of signaling through main olfactory epithelium. *Nat. Neurosci.* **6**, 519-525.

Vassalli, A., Rothman, A., Feinstein, P., Zapotocky, M. and Mombaerts, P. (2002). Minigenes impart odorant receptor-specific axon guidance in the olfactory bulb. *Neuron* **35**, 681-696.

Vassar, R., Chao, S. K., Sitcheran, R., Nunez, J. M., Vosshall, L. B. and Axel, R. (1994). Topographic organization of sensory projections to the olfactory bulb. *Cell* **79**, 981-991.

Wang, F., Nemes, A., Mendelsohn, M. and Axel, R. (1998). Odorant receptors govern the formation of a precise topographic map. *Cell* **93**, 47-60.

Wei, J., Zhao, A. Z., Chan, G. C., Baker, L. P., Impey, S., Beavo, J. A. and Storm, D. R. (1998). Phosphorylation and inhibition of olfactory adenylyl cyclase by CaM kinase II in Neurons: a mechanism for attenuation of olfactory signals. *Neuron* **21**, 495-504.

Wong, S. T., Trinh, K., Hacker, B., Chan, G. C., Lowe, G., Gaggar, A., Xia, Z., Gold, G. H. and Storm, D. R. (2000). Disruption of the type III adenylyl cyclase gene leads to peripheral and behavioral anosmia in transgenic mice. *Neuron* **27**, 487-497.

Wong, S. T., Baker, L. P., Trinh, K., Hetman, M., Suzuki, L. A., Storm, D. R. and Bornfeldt, K. E. (2001). Adenylyl cyclase 3 mediates prostaglandin E(2)-induced growth inhibition in arterial smooth muscle cells. *J. Biol. Chem.* **276**, 34206-34212.

Yoshida, T., Ito, A., Matsuda, N. and Mishina, M. (2002). Regulation by protein kinase A switching of axonal pathfinding of zebrafish olfactory sensory neurons through the olfactory placode-olfactory bulb boundary. *J. Neurosci.* **22**, 4964-4972.

Yu, C. R., Power, J., Barnea, G., O'Donnell, S., Brown, H. E., Osborne, J., Axel, R. and Gogos, J. A. (2004). Spontaneous neural activity is required for the establishment and maintenance of the olfactory sensory map. *Neuron* **42**, 553-566.

Zhao, H. and Reed, R. R. (2001). X inactivation of the OCNC1 channel gene reveals a role for activity-dependent competition in the olfactory system. *Cell* **104**, 651-660.

Zheng, C., Feinstein, P., Bozza, T., Rodriguez, I. and Mombaerts, P. (2000). Peripheral olfactory projections are differentially affected in mice deficient in a cyclic nucleotide-gated channel subunit [In Process Citation]. *Neuron* **26**, 81-91.

Zou, D. J., Feinstein, P., Rivers, A. L., Mathews, G. A., Kim, A., Greer, C. A., Mombaerts, P. and Firestein, S. (2004). Postnatal refinement of peripheral olfactory projections. *Science* **304**, 1976-1979.